Engineering properties of crumb rubber alkali-activated mortar reinforced with recycled steel fibres

Hui Zhong, Ek Whye Poon, Kenneth Chen, Mingzhong Zhang*

Department of Civil, Environmental and Geomatic Engineering, University College London, London WC1E 6BT, UK

Abstract: To mitigate the potential problems of waste tyres and Portland cement greenhouse gas emissions while further promote the sustainable development of construction industry, this paper, for the first time, explores the workability and mechanical properties of crumb rubber alkali-activated fly ash-slag mortar reinforced with recycled tyre steel fibre (RSFRAM) considering different contents of crumb rubber (CR, i.e. 5%, 10% and 15% replacement by volume of fine aggregate) and recycled tyre steel fibre (RTSF, i.e. 0.5% and 1.0% by volume). The results indicate that the inclusion of CR led to a 4.7% to 26.7% improvement in workability of RSFRAM when the RTSF content was low, while the addition of RTSF compensated the strength loss caused by the addition of CR. The combination of CR and RTSF created a synergistic effect on the flexural behaviour of RSFRAM. The optimal mixture was regarded as R5F1.0 (5% CR replacement and 1.0 vol.% RTSF) exhibiting comparable compressive strength, and superior flexural strength (around 171.1% higher), toughness indices (highest among all RSFRAMs) and residual strength factors (higher than 100) compared to the reference mixture without CR and RTSF. In addition, R5F1.0 can meet the strength requirement of concrete (i.e. 28 MPa for basic construction application) and thus suitable for structural applications as a sustainable material.

Keywords: Alkali-activated material; Rubberised concrete; Recycled fibre; Strength; Toughness

1. Introduction

Every year, more than 500 million end-of-life tyres are disposed to landfills without any secondary usage (Thomas and Gupta, 2016), which poses several threats to the society and environment, e.g. formation of deadly diseases, potential fire threat to surrounding environment, and water and soil pollution (Ramarad et al., 2015; Thomas and Gupta, 2016). The potential problems of discarded tyres motivated many researchers to find their alternative usage while the incorporation of the materials extracted from the waste tyres into cementitious materials is one of recent attempts.

* Corresponding author. Tel: +44 (0)20 7679 7299. E-mail address: mingzhong.zhang@ucl.ac.uk (M. Zhang)

Crumb rubber (CR) extracted mainly via the shredding process of waste tyres is used to partially or fully replace fine aggregates in conventional concrete, which can help improve the resistance of concrete to abrasion, impact, alkali-silica reaction and freeze-thaw cycles as well as other durability performance (Aiello and Leuzzi, 2010; Angelin et al., 2017; Liu et al., 2012; Medina et al., 2017; Si et al., 2018; Thomas and Gupta, 2016; Thomas et al., 2016). However, the main binder component of these crumb rubber concrete (CRC) is still ordinary Portland cement (OPC), which largely hinders the sustainable development of construction industry. Given the fact that the massive production of OPC accounts for approximately 8% of global CO_2 emission (Luukkonen et al., 2018), an increasing number of studies is seeking alternative binder to OPC for concrete. Alkali-activated material (AAM) is considered as a potential alternative mainly owing to its low CO_2 emission and better engineering properties compared to OPC concrete (Ding et al., 2016; Luukkonen et al., 2018; Provis, 2017). Among all AAMs, alkali-activated fly ash-slag (AAFS) system is the most promising one as it not only can mitigate the key issues of alkali-activated fly ash (AAF) and alkali-activated slag (AAS) systems such as low early-age strength and large energy consumption for AAF due to necessary heat curing and low workability, rapid setting and large shrinkage for AAS, but also it exhibits superior engineering properties under ambient temperature (Fang et al., 2018; Lee and Lee, 2013; Tu et al., 2019). Combining AAM and recycled tyre materials is a promising approach to significantly improve the sustainability of construction material and mitigate the generated environmental issues.

Up to now, several studies have reported the effect of CR on engineering properties of AAM. Dehdezi et al. (2015) explored the microstructure and physical, mechanical and dynamic properties of lightweight AAF incorporating CR, and found that partially replacing fine aggregates by CRs in AAF can improve its impact strength and resistance to cracking under impact loading. Gandoman and Kokabi (2015) demonstrated pronounced improvement of sound absorption property and noise reduction coefficient in metakaolin-based AAM containing CR compared to conventional CRC. Park et al. (2016) investigated the feasibility of applying CR in AAF and illustrated that an appropriate content of CR can be replaced with an equal volume of fine aggregates. Wongsa et al. (2018) studied the effect of CR on mechanical and thermal properties of AAF and concluded that AAF incorporated 100% CR demonstrated better thermal insulation. The effect of different CR replacement ratios for natural aggregate on mechanical and impact properties of AAS was recently estimated by Aly et al. (2019) who found that the proposed AAS incorporating CR can be used in structural elements

subjected to dynamic loading. However, significant reductions in compressive and flexural strength (e.g. up to around 93% reduction depending on the replacement ratio of CR) were observed in either OPC or AAM containing CR (Aly et al., 2019; Dehdezi et al., 2015; Gandoman and Kokabi, 2015; Park et al., 2016; Thomas and Gupta, 2016; Wongsa et al., 2018).

To compensate for the strength loss caused by CR while maintaining its generated positive impact to the resultant composite, manufactured steel fibres were usually incorporated into CRC, the addition of which enhanced the overall mechanical properties of CRC (AbdelAleem and Hassan, 2018; Fu et al., 2019; Ismail and Hassan, 2017a; Liu et al., 2012; Noaman et al., 2016; Noaman et al., 2017). In recent years, recycled tyre steel fibre (RTSF) was introduced into cementitious materials to maximise the usage of recycled materials and further promote the sustainable development. The effect of RTSF on mechanical and durability performances of fibre reinforced concrete (FRC) has been extensively investigated (Aiello et al., 2009; Bjegovic et al., 2014; Centonze et al., 2012; Frazão et al., 2019; Grzymski et al., 2019; Neocleous et al., 2008; Skarżyński and Suchorzewski, 2018; Zamanzadeh et al., 2015). However, very limited study can be found in literature regarding the effect of RTSF on the properties of CRC. For instance, Medina et al. (2017) explored the mechanical and thermal properties of CRC reinforced with RTSF and found that the addition of RTSF into CRC improved its mechanical performance and toughness because of the fibre bonding with the concrete matrix, which is consistent with the findings by Alsaif et al. (2018) that adding either manufactured or recycled steel fibres substantially mitigated the strength loss caused by the CR inclusion and further enhanced the flexural performance of CRC. In order to improve the sustainability of construction material with reducing production cost (i.e. maximise the usage of recycled materials, which can help mitigate the environmental issues), it is essential to combine AAM, CR and RTSF together. Nevertheless, until now, no relevant research has been done on the properties of AAM incorporating both CR and RTSF.

This paper, for the first time, presents an experimental study on workability and mechanical properties of crumb rubber alkali-activated fly ash-slag mortar reinforced with recycled tyre steel fibre (RSFRAM) considering different contents of CR (i.e. 5%, 10% and 15% by volume of fine aggregates) and RTSF (i.e. 0.5% and 1.0% by volume, vol.%). Firstly, the effects of CR and RTSF on workability and compressive strength were evaluated through a series of tests. Subsequently, flexural behaviour including load-deflection curve, flexural toughness and residual strength factor was estimated considering different standards. Digital microscope was used to detect the bonding

between the fibre and the matrix. Finally, several potential applications of the investigated material with an environmental analysis were discussed.

2. Experimental program

2.1 Raw materials

Class F fly ash (FA) and ground granulated blast-furnace slag (GGBS) were used as the precursors of AAFS in this study (see **Fig. 1**a and b), the chemical compositions of which are listed in **Table 1**. The mean particle size of FA and GGBS is 26.81 and 14.77 μm, respectively. The alkaline activators used in this study were 10 M sodium hydroxide (SH) and sodium silicate (SS) with silicate modulus (SiO_2 to Na_2O) of 2.0. Modified polycarboxylate-based superplasticisers (SPs) with a pH value ranging from 4 to 5 were used whist mixing to improve the flowability of RSFRAM.

CR recycled from waste tyres and Thames valley sand were used as fine aggregates (see **Fig. 1**c, d, e and f). The particle size distributions of CR and sand are shown in **Fig. 2**. The CR particles were classified into three groups according to their particle diameters (2-6 mm, 12 mesh/1.68mm, and 30 mesh/0.595 mm) and mixed using a proportion of 10%, 50%, and 40% by weight, respectively. This proportion determined as the best match to the particle size distribution of sand (see **Fig. 2**), was derived through sieve analysis as per ASTM D5644 (2018). Whilst mixing, CR and sand were used in statured surface dry (SSD) condition. Fibre adopted in this study was RTST provided by Twincon Ltd (see **Fig. 3**). The distribution of fibre length and aspect ratio is shown in **Fig. 4** (Hu et al., 2018). The physical and mechanical properties of RTST are listed in **Table 2**.

2.2 Mix proportions and sample preparation

Table 3 presents the mix proportions of all mixtures investigated in this study. The ratio of FA to GGBS ratio (20:80), alkaline to binder ratio (0.4), content of SPs (1.0% by mass of binder) were selected based on previous research (Fang et al., 2018) and set as constant. The studied parameters were content of CR and RTSF. CR particles were used as partial volume replacement for sand at four replacement levels (0%, 5%, 10%, 15%). As reinforcement, RTSFs were added into the mix at 0.5 vol.% and 1.0 vol.%. Regarding the symbols shown in **Table 3**, ‘R’ and ‘F’ represent CR and RTSF, while the denoted number stands for the content of CR or RTSF. For example, R0F0 was denoted as the reference mixture without any CR and RTSF inclusions.

Regarding the mixing procedure, FA, GGBS, CR and sand were first dry mixed for 180 s in a Cumflow concrete mixer to achieve uniform distribution. SS, SH and SPs were then added and mixed

for another 360 s. During this period, RTSTs were gradually and slowly added into the mixture to ensure uniform fibre distribution and avoid fibre-balling behaviour. After that, each mix of fresh mortar was cast into six 100 mm cubic moulds and three 100 × 100 × 350 mm prismatic moulds. The mixed fresh mortar was compacted using a vibrating table and then immediately covered with polyethylene sheets to prevent excessive loss of moisture. The covered samples were kept under a laboratory temperature of 20 ± 2˚C and demoulded after 24 h. The demoulded samples were then stored in a room maintained at an ambient temperature of 20 ± 2˚C and relative humidity of 50 ± 1% until their testing age.

2.3 Testing methods

2.3.1 Workability

Flow table tests of ASTM C1437 (2015) were conducted to determine the workability of the mixtures. The flow value was measured using a flow mould of 100 base diameter, 50 mm height, and 70 mm top opening. After mortar was cast into the mould, the table was dropped 25 times in 15 s immediately after the removal of the mould. The spread diameter of the mortar was measured at least twice in perpendicular directions.

2.3.2 Compressive strength

Six 100 mm cubes of 7-d and 28-d ages were crushed to failure using a compression testing machine with a loading rate of 6000 N/s as per BS EN 12390-3 (2009). The strength was reported by averaging the results of three cubes for each test age.

2.3.3 Flexural behaviour

Three 28-d prismatic samples for each mix were loaded under four-point bending on a 300 mm span using a universal testing machine according to ASTM C1609 (2012). A constant displacement rate of 1 mm/min was set. The modulus of rupture (i.e. flexural strength) of each mixture can be calculated using the following equation:

$$f_p = \frac{FL}{bd^2} \quad (1)$$

where f_p is the modulus of rupture of each specimen (MPa), F is the load indicated by the testing machine (kN), L is the test span of the specimen (300 mm), b is the width of the specimen (100 mm), and d is the depth of the specimen (100 mm).

In terms of flexural toughness, T_{150}^{D}, it was defined as the area under load-deflection curve up to

a midspan deflection of $L/150$, which corresponds to 2 mm for a 300 mm span length. As per ASTM C1018 (ASTM C1018, 1997), toughness indices I_5, I_{10} and I_{20} can be derived using Eqs. 2-4.

$$I_5 = \frac{A_2}{A_1} \tag{2}$$

$$I_{10} = \frac{A_3}{A_1} \tag{3}$$

$$I_{20} = \frac{A_4}{A_1} \tag{4}$$

where A_1, A_2, A_3, and A_4 correspond to area under the load-deflection curve up to 1, 3, 5.5 and 10.5 times the first-crack deflection.

The residual strength factor, $R_{5,10}$ and $R_{10,20}$, can be calculated using Eqs. 5 and 6, respectively according to ASTM C1018 (1997).

$$R_{5,10} = 20(I_{10} - I_5) \tag{5}$$

$$R_{10,20} = 10(I_{20} - I_{10}) \tag{6}$$

Digital microscope (Dino-Lite Edge AM73115MZT) was applied to study the fracture zone of the failed samples with the aim of observing the bonding between the fibre and the matrix.

3. Results and discussion

3.1 Workability

In this study, the flow value was used to reflect the workability of fresh mixtures. A higher flow value represents higher fluidity and mobility and better workability). **Fig. 5** shows the effects of CR and RTSF on the flow value of all mixtures where R0F0 is the reference mixture without addition of both CR and RTSF. It can be observed that the inclusion of CR improved the workability of RSFRAM, whereas the addition of RTSF reduced its workability accordingly. The effects of CR and RTSF on workability are discussed in detail below.

3.1.1 Effect of CR

In general, the flow value of RSFRAM was improved with the increase of CR replacement ratio, which was found to be more pronounced when the RTSF addition was lower. With the presence of 0.5 vol.% RTSF, the flow value of RSFRAM was increased by 3.9% and 25.7% when the CR replacement ratio changed from 5% to 10% and 15%, respectively. Similarly, when the CR replacement ratio increased from 5% to 10%, the flow value of RSFRAM containing 1.0 vol.% RTSF was enhanced by 39.5%. The improved workability caused by the CR addition can be attributed to the reduced surface friction between CR and other constituent materials whist mixing, owing to the

relatively smoother surface texture of CR in comparison with sand particles. However, further addition of CR content slightly reduced the flow value of RSFRAM incorporating 1.0 vol.% RTSF (i.e. decreased by approximately 3.3%), which can be ascribed to the increased inter-particle friction when having too many constituents in the mix (Abaza and Hussein, 2015). Compared to R0F0, the fibre incorporation induced a more significant influence on the workability. As shown in **Fig. 5**, all RSFRAMs containing 0.5 vol.% RTSF possessed comparable or higher workability as compared with R0F0 (i.e. ranging from 4.7% to 26.7%), whereas the flow values of all RSFRAMs containing 1.0 vol.% RTSF were generally lower than that of R0F0, which proved that the positive influence in workability resulted from the CR incorporation could be reduced after adding RTSF.

3.1.2 Effect of RTSF

It can be clearly seen from **Fig. 5** that the inclusion of RTSF resulted in an adverse effect on the workability of RSFRAM. Due to the flow-enhancing effect of CR, R5F0.5 exhibited comparable flow value to R0F0. Apart from this, the flow value of RSFRAM incorporating 5%, 10% and 15% CR was decreased by 33.0%, 10.0% and 27.9% when the RSTF content increased from 0.5 vol.% to 1.0 vol.%. The reduced workability due to fibre incorporation is mainly as a result of the increased shear resistance to the flow of fresh mixtures with relatively higher viscosity. In addition, the RTSF with a large surface area induced a tendency for agglomeration leading to further reduction in workability (Alsaif et al., 2018). Nevertheless, it is worth mentioning that no significant fibre balling effect was observed whilst mixing, regardless of CR replacement ratio. As a consequence, the utilization of RSFRAM incorporating 15% CR content (by volume) and 1.0 vol.% RTSF is unlikely to raise issues with the handling, placing and finishing in structural applications.

3.2 Compressive strength

It is generally agreed that the incorporation of CR would accordingly reduce the compressive strength of concrete and thus, it is critical to assess the effects of both CR and RTSF on the compressive strength of RSFRAM with different curing ages. The effects of CR and RTSF on the compressive strength of all mixtures at 7 and 28 d are illustrated in **Fig. 6**. Generally, the 7-d compressive strength of all mixtures ranged from 15.0 to 21.3 MPa while the compressive strength at 28 d was in the range of 22.6-35.8 MPa.

3.2.1 Effect of CR

As shown in **Fig. 6**, independent of curing age, the compressive strength of RSFRAM was decreased

with increasing CR replacement ratio. When the CR replacement ratio changed from 0% to 15%, the 7-d and 28-d compressive strength of all RSFRAMs (except R5F1.0) was reduced by around 7.5% to 29.6% (see **Fig. 6**a) and 7.5% to 36.9% (see **Fig. 6**b), respectively, as compared with the reference mixture. RSFRAM incorporating 15% CR (by volume) achieved the lowest compressive strengths (i.e. 15.0 MPa and 22.6 MPa at 7 d and 28 d, respectively) implying that 15% CR replacement ratio significantly weakened the compressive strength. The reduction in compressive strength here is consistent with previous studies on AAM (Aly et al., 2019; Dehdezi et al., 2015; Park et al., 2016; Wongsa et al., 2018) that the compressive strength of AAM incorporating CR was reduced in different extents (up to 35.0% reduction) based on different CR replacement ratios.

The reasons causing the strength reduction are similar to that in normal concrete incorporating CR, and can be explained as follows (Alsaif et al., 2018; Aly et al., 2019; Chen et al., 2019; Dehdezi et al., 2015; Fu et al., 2019; Turatsinze et al., 2007): (1) the hydrophobic nature (i.e. water-repelling) of CR particles results in poor bonding with the AAFS matrix leading to a weak interfacial transition zone; (2) the elastic modulus of CR is much lower than that of sand, which causes larger deformation and higher stress concentration in the vicinity of CR particles accelerating the compressive failure; (3) the incorporation of CR increases the non-homogeneity of RSFRAM due to the low specific gravity of CR; (4) the CR particles tend to entrap air whilst mixing, which increases the porosity of RSFRAM. However, R5F1.0 possessed nearly identical compressive strength as compared with R0F0 (no more than 0.1 MPa difference), which implies that the inclusion of RTSF compensated the strength loss caused by the CR addition.

3.2.2 Effect of RTSF

As seen in **Fig. 6**, considering the same CR replacement ratio, the compressive strengths of RSFRAMs at 7 and 28 d were significantly enhanced by altering the RTSF dosage from 0.5 vol.% to 1.0 vol.%. For instance, at the CR replacement ratio of 5%, the 7-d and 28-d compressive strength was increased by approximately 11.0% and 8.2%, respectively. In addition, it is worth noting that the 28-d compressive strength of RSFRAM containing 15% CR (by volume) increased the most (around 37.2%) when the RTSF content increased to 1.0 vol.%, which in turn supports the previous discussion that the compressive strength was significantly decreased by replacing 15% sand with CR (by volume). The observed enhancement in compressive strength due to fibre addition is in good agreement with the previous studies (Guo and Pan, 2018; Khan et al., 2018; Sukontasukkul et al.,

2018) that the incorporation of a certain content of steel fibre effectively increased the compressive strength of AAM. This can be mainly accredited to the hydrophilic nature of steel fibre (Ranjbar et al., 2016), which significantly improves the bond between the fibre and the matrix resulting in improvement in strength. Besides, RTSF with a high elastic modulus (see **Table 2**) facilitates the stress dispersion throughout the matrix restraining the formation of tensile cracks (Ismail and Hassan, 2017b). As a consequence, the load-carrying capacity of RSFRAM is accordingly improved.

It is noteworthy that all mixtures, apart from R15F0.5, exceeded the minimum compressive strength of 28 MPa for basic engineering application (see **Fig. 6**b), as stated by ACI 318-05 (2005), which suggests that the incorporation of 1.0 vol.% RTSF can efficiently compensate the strength loss caused by the CR inclusion in AAFS ensuring sufficient strength properties for future application.

3.3 Flexural behaviour

3.3.1 Load-deflection curve

Fig. 7 illustrates three typical stages of load-deflection curve for FRC, which consists of elastic stage up to the appearance of the first crack, deflection-hardening stage and deflection-softening stage after reaching the peak load. **Fig. 8** shows the load-deflection curve of all mixtures under four-point bending at 28 d. It can be observed that the reference mixture failed at the elastic stage owing to the lack of fibre reinforcement. All RSFRAMs exhibited a conspicuous trend like that shown in **Fig. 7**.

In the elastic stage, the deflection at the first-crack (δ_{LOP}) varied from 0.26 mm (R0F0) to 1.22 mm (R15F0.5) implying that higher δ_{LOP} values were obtained at higher CR replacement. The δ_{LOP} value of R15F0.5 was enhanced by around 41.9% and 32.6% compared to R10F0.5 and R5F0.5, respectively. With the presence of 1.0 vol.% RTSF, the δ_{LOP} value of R5F1.0 and R10F1.0 was about 296.2% and 319.2% higher in comparison with R0F0. However, with the further addition of CR content (i.e. 15% CR by volume), the δ_{LOP} value was reduced to around 0.61 mm suggesting that, the upper limit point for CR replacement ratio was 10%. Beyond this point, the elastic performance of RSFRAM in flexural bending would accordingly diminish. Furthermore, the presence of RTSF did not have significant impact on δ_{LOP}. Similar to compressive strength, the inclusion of CR into AAFS decreased its load at the first crack (F_{LOP}), whereas the incorporation of RTSF accordingly improved the first-crack load, which is in consistence with the previous study (Fu et al., 2019).

The incorporation of CR did not induce a significant influence on deflection-hardening behaviour of RSFRAM while increasing the RTSF dosage prolonged the deflection-hardening stage (e.g.

R5F1.0 exhibited longer deflection-hardening region than R5F0.5). **Fig. 9** presents the effects of CR and RTSF on the 28-d flexural strength of all mixtures. The combined CR and RTSF significantly improved the flexural strength of RSFRAM as compared with the reference mixture. By assessing the effect of CR inclusion, the flexural strength of RSFRAM containing 0.5 vol.% RTSF was decreased from 3.92 MPa to 3.55 MPa when the CR replacement ratio changed from 5% to 15%. No obvious negative reduction was observed when the CR replacement ratio altered from 5% to 10% (only 0.02 MPa lower). Similar phenomenon was identified in the presence of 1.0 vol.% RTSF, where the flexural strength was reduced by around 25.6% when the CR replacement ratio changed from 5% to 10%. These findings are consistent with previous studies (Aly et al., 2019; Dehdezi et al., 2015) that replacing 20% fine aggregate with CR by volume decreased the flexural strength by about 30.0%, which can be also attributed to the less cohesion force between the CR and the matrix resulting in quicker localised failure. Nevertheless, the negative influence on flexural strength caused by the CR addition can be mitigated by the presence of RTSF. As seen in **Fig. 8**, RTSF content had a major incremental effect on the peak load (F_p). R5F1.0 achieved the highest F_p of 21.8 kN, which was 242.2% and 63.7% higher than that of R0F0 and R5F0.5, respectively. This suggests that RTSF played a dominated role in resisting the crack development across the fracture zone because of fibre bridging action, especially when more RTSFs are perpendicular to the crack surface (Yousefieh et al., 2017; Zhou and Uchida, 2017) indicating the importance of fibre orientation within the mixture. R5F1.0 also attained the highest flexural strength of 6.29 MPa (see **Fig. 9**). It is worth noting that all RSFRAMs consistently possessed higher flexural strength (at least 53.0% higher) than R0F0 while RSFRAMs containing 1.0 vol.% RTSF had up to 60.5% higher flexural strength as compared with RSFRAMs with 0.5 vol.% RTSF. If solely considering the flexural performance before the peak load, R5F1.0 can be regarded as the optimal mixture.

The strain softening stage is visualised through the gradient of the descending branch in each load-deflection curve, which symbolises the rate of reduction in residual strength with increasing strain. It can be seen from **Fig. 8** that, R5F0.5 achieved the highest ultimate deflection of about 12.6 mm, which substantially outperformed the reference mixture (i.e. only 0.26 mm) illustrating its good energy absorption capacity among other RSFRAMs. Under the same fibre dosage, no clear trend can be identified for the effect of CR on the deflection-softening behaviour. However, increasing the CR replacement ratio slightly altered the shape of the descending branch, which was found to be flatter,

showing good agreement with the findings by Alsaif et al. (2018). However, increasing the RTSF content from 0.5 vol.% to 1.0 vol.% slightly shortened the deflection-hardening stage and decreased the ductility of RSFRAM, which is in line with the previous study (Fu et al., 2019) that the strain-hardening behaviour of concrete incorporating CR was negatively affected by increasing the steel fibre content due to the intrinsic brittle nature of high-modulus fibre (Pakravan et al., 2017).

The improvement in flexural performance due to fibre incorporation can be also explained through analysing the failure mode of RSFRAM, which is shown in **Fig. 10**. The addition of RTSF contributed to the reduced width of macro-cracks indicating the synergetic effect between CR and RTSF in restraining the crack propagation. The formation of derivative cracks may also prolong crack paths and increase the area of the failure surface (see the right image of **Fig. 10**), which leads to stress relaxation while potentially improving the crack-arresting mechanism of RTSF.

3.3.2 Flexural toughness

Flexural toughness is a good indicator of energy absorption capacity for concrete. Sufficient toughness is essential for structural applications, which can provide more obvious warning before failure instead of sudden brittle failure. Since R0F0 failed very quickly at the deflection of around 0.26 mm, its toughness was considered as 0. The flexural toughness of all RSFRAMSs according to ASTM C1609 (2012) is illustrated in **Fig. 11**. It can be clearly seen that, under the same fibre dosage, increasing the CR replacement ratio did not induce a dramatic impact on the flexural toughness. For RSFRAM containing 0.5 vol.% RTSF, the flexural toughness was improved slightly by 5.5% when the CR replacement ratio changed from 5% to 10%, whereas with the further addition of CR (i.e. 15% by volume), the flexural toughness was decreased by about 7.1%. This supports the previous discussion that 10% CR replacement ratio can be considered as the upper limited ratio in AAFS system. Similar findings were observed for RSFRAM containing 1.0 vol.% RTSF. However, the inclusion of RTSF dramatically improved the flexural toughness, with an increase of up to 56.4% when changing the RTSF content from 0.5 vol.% to 1.0 vol.%, which is consistent with the previous study (Ahmadi et al., 2017) that adding 1.0 vol.% RTSF into normal concrete enhanced its flexural toughness. This can be primarily ascribed to the fibre bridging action across the cracking zone, which dissipates a large amount of energy.

The toughness indices shown in **Fig. 12** based on ASTM C1018 (1997) provide a relative indicator of deflection-hardening or deflection-softening behaviour for FRC (Shaikh and Hosan, 2016). As

seen in **Fig. 12**, each RSFRAM had I_5, I_{10} and I_{20} values above 5, 10 and 20, respectively, which indicates its deflection-hardening ability regardless of CR replacement ratio, which agrees well with the findings by Ranjbar et al. (2016) that the toughness indices of AAF was significantly improved by adding micro-steel fibres. An increase in CR replacement ratio was accompanied with a decrease in toughness index. It was found that CR and RTSF did not appear to have a consistent influence on I_5, where higher CR replacement ratio conspicuously decreased toughness indices. For instance, R5F0.5, R10F0.5 and R15F0.5 had I_{10} values of 18.3, 17.9 and 12.8, along with I_{20} values of 37.1, 32.7 and 22.8, respectively. The weak bonding between CR and AAFS matrix led to reduced flexural strength while failure often occurred with the formation of localised micro-cracks adjacent to CR particles. In addition, low stiffness and high Poisson's ratio of CR resulted in an accelerated contraction of rubber in the lateral direction, facilitating debonding (Guo et al., 2014).

Nevertheless, it is worth noting that RTSF exhibited a toughness-enhancing potential. Averagely, a 0.5 vol.% increase in RTSF addition corresponds to a 2.08 and 4.61 increase in I_{10} and I_{20}, respectively, which are in good agreement with findings by previous studies (Caggiano et al., 2017; Sengul, 2016) that the incorporation of RTSF induced a substantial enhancement in post-cracking toughness of FRC. The pronounced contribution of RTSF to overall strength of RSFRAM was enabled by a combination of fibre bridging across cracks and a strong bond formed between RTSF and AAFS matrix. As shown in **Fig. 13**, the reinforcing mechanism of RTSF plays a critical role in sustaining loads after first-crack through fibre-bridging action (see **Fig. 13**a). For RSFRAM, an additional amount of energy was required to pull out the fibres across the cracking zone in order to completely fracture the specimen, which consequently leads to improvement in post-cracking toughness (see **Fig. 13**b). However, high scatter in toughness indices for some specimens (particularly R10F0.5) can be observed. This can be explained by the non-uniform dimension of RTSF, as shown in **Fig. 3**, which would drastically influence the crossing of fibres along crack openings and in turn result in significant variations in the bridging mechanism. RTSF with more irregular shape has higher possibility to be ruptured during fibre-bridging action owing to greater fibre pull-out load and the toughness properties would be accordingly influenced (Frazão et al., 2019).

The trend observed from the flexural toughness based on ASTM C1609 (2012) was found to be similar to that of I_5 derived in accordance with ASTM C1018 (1997). Nevertheless, as stated by Kim et al. (2011), the point *L/150* (i.e. 2 mm in this study) was not enough to accurately describe the

flexural behaviour of FRC with deflection-hardening feature. For instance, as shown in **Fig. 8,** the point *L/150* just appeared prior to the peak point for R5F1.0 implying that the calculated flexural toughness for R5F1.0 was not in the range of post-cracking behaviour. Thus, the derived toughness indices were more appropriate to describe the flexural behaviour of FRC with deflection-hardening behaviour.

3.3.3 Residual strength factor

The residual strength factor of concrete can reflects its ductility by providing a relative measure of the remaining load capacity upon the onset of cracks (Noushini et al., 2018). In general, $R_{5,10}$ and $R_{10,20}$ capture the residual flexural strength of RSFRAM in the deflection-hardening and deflection-softening stages, respectively. It can be seen from **Fig. 14** that nearly all RSFRAMs possess $R_{5,10}$ and $R_{10,20}$ values above 100, which categorises RSFRAM as a material with great plasticity (Fu et al., 2019).

The residual strength is closely related to flexural toughness and thus, similar trends were observed when CR and RTSF contents varied. The increase of CR replacement ratio was accompanied by a decrease in both $R_{5,10}$ and $R_{10,20}$ values. For instance, the $R_{5,10}$ value of R5F0.5, R10F0.5 and R15F0.5 was 229.2, 215.1 and 146.5, respectively, indicating the similar finding that adding 15% CR (by volume) significantly weakened the post-cracking behaviour of RSFRAM. This observation is in line with findings by Mohammadi and Khabbaz (2015), who found a significant decrease in residual load at the net deflection of 0.5 mm for normal concrete when the CR replacement ratio changed from 20% to 40%. On the other hand, increasing RTSF dosage at low CR replacement ratio improved residual strengths, with R5F1.0 showing the highest $R_{5,10}$ and $R_{10,20}$ values of 286.3 and 234.8, respectively. Nevertheless, the residual strength improvement of RTSF was less effective at higher CR replacement ratio, with R10F1.0 exhibiting a slight decrease in residual strength factors as compared with R10F0.5 (i.e. around 13%). This could be also attributed to the non-uniform dimension of RTSF, which might affect the internal structure of RSFRAM leading to reduced performance (Grzymski et al., 2019). This can be observed from **Fig. 15** that ruptured RTSFs in the failed plane were mostly twisted and irregular in shape.

4. Potential applications

CRC processes several better characteristics over conventional concrete, such as lightweight, superior impact behaviour, higher resistance to cracking, anti-aging, anti-permeability and better sound

absorption and thermal properties (Liu et al., 2012; Medina et al., 2017; Si et al., 2018; Thomas and Gupta, 2016; Wongsa et al., 2018). Given these excellent properties, CRC is promising to be used for pavements and barriers that may suffer from serious dynamic impact, foundation pad for railway stations, and also as sound absorbers (Fu et al., 2019; Wongsa et al., 2018). Additionally, it was reported that AAM containing CR can be used for structural elements under dynamic loading (Aly et al., 2019).

The incorporation of CR into concrete reduces its overall strength properties, while the inclusion of steel fibre can mitigate this drawback. The improved performance make steel fibre reinforced CRC promising to be used for pavements and overlays (Noaman et al., 2017). Moreover, the strength loss in CRC can be mitigated when CR is pre-treated with sodium hydroxide solution owing to reduced porosity (Guo et al., 2017; Ma and Yue, 2013; Si et al., 2017), implying that the use of CRC activated by alkaline activators can in turn overcome the issue of strength reduction for conventional CRC.

In this study, R5F1.0 can be regarded as the optimal mixture, as its compressive strength and flexural properties were the highest among other RSFRAMs. According to ACI 318-05 (2005), the 28-d compressive strength of concrete should be higher than 28 MPa for basic construction purposes and R5F1.0 can satisfy this requirement (i.e. 35.8 MPa at 28 d). The flexural strength of R5F1.0 was 6.29 MPa, which was 171.1% higher than that of reference mixture (R0F0). Obvious deflection-hardening behaviour was observed for R5F1.0 under bending indicating its superior ductility. The residual strength factors of R5F1.0 were the highest among other RSFRAMs (i.e. 286.3 and 234.8 for $R_{5,10}$ and $R_{10,20}$, respectively), which were both higher than 100 illustrating its very high plasticity. To sum up, considering the compressive strength and flexural behaviour, R5F1.0 can be used for structural elements as well as pavements and flooring that require high ductility and good performance to resist loads and cracking.

In 2016, the estimated CO_2 emission released from the manufacture of OPC was around 1.45 Gt, accounting for approximately 8% of the total CO_2 release globally (Luukkonen et al., 2018). Moreover, the demand of OPC will be gradually increased year by year (i.e. about 3.64-4.38 Gt per year by 2050) (Schneider et al., 2011), which would result in a number of environment issues (e.g. global warming). The utilization of AAM can significantly reduce the global CO_2 emission produced by the cement industry, i.e. around 55-75% lower relative to the production of OPC depending on the type and content of alkali-activator used (Yang et al., 2013). More specifically, it was found that

producing 1 t of AAM releases at most 0.24 t CO_2, which was about 60% lower compared to the manufacture of OPC (Zhang et al., 2017). Furthermore, the cost of producing 1 m^3 of AAFS can be as low as £41.72, i.e. 19% lower relative to the manufacture of OPC (Liu et al., 2019), implying that AAFS can be treated as cost-effective and environmentally friendly binder material for concrete. On the other hand, approximately 1000 million end-of-life tyres are generated annually and a half (i.e. 500 million) is sent to landfill as garbage, while this number would continuously increase (i.e. about 1200 million by the year of 2030) (Thomas and Gupta, 2016). The accumulated waste tyres would induce serious issues to the environment and human society, e.g. potential fire and disease sources (Ramarad et al., 2015). Additionally, the manufactured fibres used for the reinforcement in concrete (e.g. steel and polypropylene fibres) emits a large amount of energy accounting for around 15% of the total building energy (Chen et al., 2019). This amount could be reduced by utilizing the recycled materials (Gao et al., 2001). Through several processing phases (e.g. extraction and shredding, granulating, pulverization and separation), a number of materials can be recovered from the waste tyres including granule, rubber powder, steel and textile fibres (Gigli et al., 2019). It is worth noting that rubber and steel accounts for a majority of the tyres' composition (i.e. 41%-48% and 13%-27%, respectively depending on the type of tyre) (Ramarad et al., 2015). Therefore, it is crucial to properly reuse the recycled tyre materials especially rubber particles and steel fibres in order to promote the sustainable development and reduce the environmental problems. This study explored the feasibility of recycling waste products to develop a construction material with acceptable workability and better mechanical properties relative to plain AAFS. By combining AAFS, CR and RTSF together, it was found that the developed RSFRAM with appropriate contents of CR and RTSF exhibited better mechanical properties than plain AAFS, which has a great potential to mitigate the aforementioned environmental issues and reduce the corresponding production cost.

5. Conclusions

This study examined the workability and mechanical properties of crumb rubber alkali-activated fly ash-slag mortar reinforced with recycled tyre steel fibre (RSFRAM), in which crumb rubber (CR) derived from waste tyres partially replaced sand between 5% to 15% volume replacement and recycled tyre steel fibre (RTSF) was used as reinforcement at 0.5 vol.% and 1.0 vol.%. Based on the experimental results in this study, the main conclusions can be drawn as follows:

- The workability of RSFRAM was improved by increasing the CR replacement ratio when the RTSF content was low (0.5 vol.%) as compared with the reference mixture (i.e. in the range of 4.7% to 26.7%). However, as the RTSF content increased, the workability of RSFRAM was reduced by up to 32.8% compared to that of plain AAFS mortar (R0F0).
- The compressive strength of RSFRAM at different ages decreased with increasing CR content. Up to a 36.9% loss was found in R15F0.5, as compared with R0F0. Nevertheless, the strength loss can be compensated by reinforcing RTSF, in which R5F1.0 displayed comparable 28-d compressive strength relative to R0F0. Except R15F0.5, all samples exceeded 28 MPa in compressive strength and are therefore suitable for structural applications.
- A remarkable flexural performance was observed for RSFRAM (i.e. pronounced deflection-hardening feature was observed), in which the flexural strength was enhanced by up to 171.1% as compared with R0F0. The residual strength factors of RSFRAM were mostly higher than 100 showing its superior toughness.
- The optimal mixture of RSFRAM was found to be R5F1.0 if solely considering the mechanical properties. R5F1.0 exhibited comparable compressive strength (i.e. less than 0.1 MPa difference) and extraordinary flexural behaviour in comparison with the reference mixture without CR and RTSF inclusions.

The proposed material integrating AAFS, CR and RTSF is beneficial to maximise the usage of waste materials (i.e. FA, GGBS and end-of-life tyres), which can significantly mitigate the environmental issues and promote the sustainable development of construction industry. In this study, although no pronounced benefits were identified by applying CR into AAM in terms of mechanical properties, combining CR and RTSF into AAFS induced better mechanical properties especially flexural behaviour. As a consequence, a majority of recycled CR can be reused and integrated with RTSF in developing sustainable construction material. In the future, another material recycled from waste tyres, i.e. recycled tyre polymer fibre (RTPF), will be integrated with RTSF to further improve the material properties as previous studies (Baričević et al., 2018; Chen et al., 2019) found that the addition of RTPF can improve the early-age shrinkage resistance and dynamic compressive behaviour of FRC. The dynamic behaviour and durability performance of hybrid RTSF and RTPF reinforced AAFS incorporating CR will be comprehensively investigated. This is a subject of ongoing work and will be presented in a future publication.

Acknowledgements

The authors gratefully acknowledge financial support from the Engineering and Physical Sciences Research Council (EP/R041504/1 and EP/N509577/1), the Royal Society (IE150587) and the State Key Laboratory of Silicate Materials for Architectures (Wuhan University of Technology) (SYSJJ2018-08). The authors would like to thank Twincon Ltd and Hanson UK for generously providing recycled steel fibres and slag, respectively. The authors also thank Mr. Warren Gaynor, Dr. Shi Shi and Mr. Raman Mangabhai from UCL Laboratory of Advanced Materials and Dr. Judith Zhou from UCL Environmental Engineering Laboratory for their help with experiments.

References

Abaza, O.A., S. Hussein, Z., 2015. Flexural Behavior of Steel Fiber-Reinforced Rubberized Concrete. Journal of Materials in Civil Engineering 28(1), 1-10.

AbdelAleem, B.H., Hassan, A.A.A., 2018. Development of self-consolidating rubberized concrete incorporating silica fume. Construction and Building Materials 161, 389-397.

ACI 318M, 2005. Building Code Requirements for Structural Concrete and Commentary (ACI 318M-05). American Construction Institution, p. 436.

Ahmadi, M., Farzin, S., Hassani, A., Motamedi, M., 2017. Mechanical properties of the concrete containing recycled fibers and aggregates. Construction and Building Materials 144, 392-398.

Aiello, M.A., Leuzzi, F., 2010. Waste tyre rubberized concrete: properties at fresh and hardened state. Waste Manag 30(8-9), 1696-1704.

Aiello, M.A., Leuzzi, F., Centonze, G., Maffezzoli, A., 2009. Use of steel fibres recovered from waste tyres as reinforcement in concrete: pull-out behaviour, compressive and flexural strength. Waste Manag 29(6), 1960-1970.

Alsaif, A., Koutas, L., Bernal, S.A., Guadagnini, M., Pilakoutas, K., 2018. Mechanical performance of steel fibre reinforced rubberised concrete for flexible concrete pavements. Construction and Building Materials 172, 533-543.

Aly, A.M., El-Feky, M.S., Kohail, M., Nasr, E.-S.A.R., 2019. Performance of geopolymer concrete containing recycled rubber. Construction and Building Materials 207, 136-144.

Angelin, A.F., Lintz, R.C.C., Gachet-Barbosa, L.A., Osório, W.R., 2017. The effects of porosity on mechanical behavior and water absorption of an environmentally friendly cement mortar with recycled rubber. Construction and Building Materials 151, 534-545.

ASTM C1018, 1997. Standard Test Method for Flexural Toughness and First-Crack Strength of Fiber-Reinforced Concrete (Using Beam With Third-Point Loading). ASTM International, West Conshohocken, PA, United States.

ASTM C1437, 2015. Standard Test Method for Flow of Hydraulic Cement Mortar. ASTM International, West Conshohocken, PA, United States.

ASTM C1609, 2012. Standard Test Method for Flexural Performance of Fiber-Reinforced Concrete (Using Beam With Third-Point Loading). ASTM International, West Conshohocken, PA, United States.

ASTM D5644, 2018. Standard Test Method for Rubber Compounding Materials—Determination of Particle Size Distribution of Recycled Vulcanizate Particulate Rubber. ASTM International, West Conshohocken, PA, United States.

Baričević, A., Jelčić Rukavina, M., Pezer, M., Štirmer, N., 2018. Influence of recycled tire polymer fibers on concrete properties. Cement and Concrete Composites 91, 29-41.

Bjegovic, D., Baricevic, A., Lakusic, S., Damjanovic, D., Duvnjak, I., 2014. Positive Interaction of Industrial and Recycled Steel Fibres in Fibre Reinforced Concrete. Journal of Civil Engineering and Management 19, S50-S60.

BS EN 12390-3, 2009. Testing Hardened Concrete Part 3: Compressive Strength of test Specimens. BSI Standards Publication.

Caggiano, A., Folino, P., Lima, C., Martinelli, E., Pepe, M., 2017. On the mechanical response of Hybrid Fiber Reinforced Concrete with Recycled and Industrial Steel Fibers. Construction and Building Materials 147, 286-295.

Centonze, G., Leone, M., Aiello, M.A., 2012. Steel fibers from waste tires as reinforcement in concrete: A mechanical characterization. Construction and Building Materials 36, 46-57.

Chen, M., Chen, W., Zhong, H., Chi, D., Wang, Y., Zhang, M., 2019. Experimental study on dynamic compressive behaviour of recycled tyre polymer fibre reinforced concrete. Cement and Concrete Composites 98, 95-112.

Dehdezi, P.K., Erdem, S., Blankson, M.A., 2015. Physico-mechanical, microstructural and dynamic properties of newly developed artificial fly ash based lightweight aggregate – Rubber concrete composite. Composites Part B: Engineering 79, 451-455.

Ding, Y., Dai, J.-G., Shi, C.-J., 2016. Mechanical properties of alkali-activated concrete: A state-of-

the-art review. Construction and Building Materials 127, 68-79.

Fang, G., Ho, W.K., Tu, W., Zhang, M., 2018. Workability and mechanical properties of alkali-activated fly ash-slag concrete cured at ambient temperature. Construction and Building Materials 172, 476-487.

Frazão, C., Díaz, B., Barros, J., Bogas, J.A., Toptan, F., 2019. An experimental study on the corrosion susceptibility of Recycled Steel Fiber Reinforced Concrete. Cement and Concrete Composites 96, 138-153.

Fu, C., Ye, H., Wang, K., Zhu, K., He, C., 2019. Evolution of mechanical properties of steel fiber-reinforced rubberized concrete (FR-RC). Composites Part B: Engineering 160, 158-166.

Gandoman, M., Kokabi, M., 2015. Sound barrier properties of sustainable waste rubber/geopolymer concretes. Iranian Polymer Journal 24(2), 105-112.

Gao, W., Ariyama, T., Ojima, T., Meier, A., 2001. Energy impacts of recycling disassembly material in residential buildings. Energy and Buildings 33(6), 553-562.

Gigli, S., Landi, D., Germani, M., 2019. Cost-benefit analysis of a circular economy project: a study on a recycling system for end-of-life tyres. Journal of Cleaner Production 229, 680-694.

Grzymski, F., Musiał, M., Trapko, T., 2019. Mechanical properties of fibre reinforced concrete with recycled fibres. Construction and Building Materials 198, 323-331.

Guo, S., Dai, Q., Si, R., Sun, X., Lu, C., 2017. Evaluation of properties and performance of rubber-modified concrete for recycling of waste scrap tire. Journal of Cleaner Production 148, 681-689.

Guo, X., Pan, X., 2018. Mechanical properties and mechanisms of fiber reinforced fly ash–steel slag based geopolymer mortar. Construction and Building Materials 179, 633-641.

Guo, Y.C., Zhang, J.H., Chen, G., Chen, G.M., Xie, Z.H., 2014. Fracture behaviors of a new steel fiber reinforced recycled aggregate concrete with crumb rubber. Construction and Building Materials 53, 32-39.

Hu, H., Papastergiou, P., Angelakopoulos, H., Guadagnini, M., Pilakoutas, K., 2018. Mechanical properties of SFRC using blended Recycled Tyre Steel Cords (RTSC) and Recycled Tyre Steel Fibres (RTSF). Construction and Building Materials 187, 553-564.

Ismail, M.K., Hassan, A.A.A., 2017a. An experimental study on flexural behaviour of large-scale concrete beams incorporating crumb rubber and steel fibres. Engineering Structures 145, 97-108.

Ismail, M.K., Hassan, A.A.A., 2017b. Shear behaviour of large-scale rubberized concrete beams

reinforced with steel fibres. Construction and Building Materials 140, 43-57.

Khan, M.Z.N., Hao, Y., Hao, H., Shaikh, F.U.A., 2018. Mechanical properties of ambient cured high strength hybrid steel and synthetic fibers reinforced geopolymer composites. Cement and Concrete Composites 85, 133-152.

Kim, D.J., Park, S.H., Ryu, G.S., Koh, K.T., 2011. Comparative flexural behavior of Hybrid Ultra High Performance Fiber Reinforced Concrete with different macro fibers. Construction and Building Materials 25(11), 4144-4155.

Lee, N.K., Lee, H.K., 2013. Setting and mechanical properties of alkali-activated fly ash/slag concrete manufactured at room temperature. Construction and Building Materials 47, 1201-1209.

Liu, F., Chen, G., Li, L., Guo, Y., 2012. Study of impact performance of rubber reinforced concrete. Construction and Building Materials 36, 604-616.

Liu, Y., Shi, C., Zhang, Z., Li, N., 2019. An overview on the reuse of waste glasses in alkali-activated materials. Resources, Conservation and Recycling 144, 297-309.

Luukkonen, T., Abdollahnejad, Z., Yliniemi, J., Kinnunen, P., Illikainen, M., 2018. One-part alkali-activated materials: A review. Cement and Concrete Research 103, 21-34.

Ma, Q.W., Yue, J.C., 2013. Effect on Mechanical Properties of Rubberized Concrete due to Pretreatment of Waste Tire Rubber with NaOH. Applied Mechanics and Materials 357-360, 897-904.

Medina, N.F., Medina, D.F., Hernández-Olivares, F., Navacerrada, M.A., 2017. Mechanical and thermal properties of concrete incorporating rubber and fibres from tyre recycling. Construction and Building Materials 144, 563-573.

Mohammadi, I., Khabbaz, H., 2015. Shrinkage performance of Crumb Rubber Concrete (CRC) prepared by water-soaking treatment method for rigid pavements. Cement and Concrete Composites 62, 106-116.

Neocleous, K., Tlemat, H., Pilakoutas, K., 2008. Design issues for concrete reinforced with steel fibers, including fibers recovered from used tires. Journal of Materials in Civil Engineering 18, 677-685.

Noaman, A.T., Abu Bakar, B.H., Akil, H.M., 2016. Experimental investigation on compression toughness of rubberized steel fibre concrete. Construction and Building Materials 115, 163-170.

Noaman, A.T., Abu Bakar, B.H., Akil, H.M., Alani, A.H., 2017. Fracture characteristics of plain and steel fibre reinforced rubberized concrete. Construction and Building Materials 152, 414-423.

Noushini, A., Hastings, M., Castel, A., Aslani, F., 2018. Mechanical and flexural performance of synthetic fibre reinforced geopolymer concrete. Construction and Building Materials 186, 454-475.

Pakravan, H.R., Latifi, M., Jamshidi, M., 2017. Hybrid short fiber reinforcement system in concrete: A review. Construction and Building Materials 142, 280-294.

Park, Y., Abolmaali, A., Kim, Y.H., Ghahremannejad, M., 2016. Compressive strength of fly ash-based geopolymer concrete with crumb rubber partially replacing sand. Construction and Building Materials 118, 43-51.

Provis, J.L., 2017. Alkali-activated materials. Cement and Concrete Research 114, 40-48.

Ramarad, S., Khalid, M., Ratnam, C.T., Chuah, A.L., Rashmi, W., 2015. Waste tire rubber in polymer blends: A review on the evolution, properties and future. Progress in Materials Science 72, 100-140.

Ranjbar, N., Talebian, S., Mehrali, M., Kuenzel, C., Cornelis Metselaar, H.S., Jumaat, M.Z., 2016. Mechanisms of interfacial bond in steel and polypropylene fiber reinforced geopolymer composites. Composites Science and Technology 122, 73-81.

Schneider, M., Romer, M., Tschudin, M., Bolio, H., 2011. Sustainable cement production—present and future. Cement and Concrete Research 41(7), 642-650.

Sengul, O., 2016. Mechanical behavior of concretes containing waste steel fibers recovered from scrap tires. Construction and Building Materials 122, 649-658.

Shaikh, F.U.A., Hosan, A., 2016. Mechanical properties of steel fibre reinforced geopolymer concretes at elevated temperatures. Construction and Building Materials 114, 15-28.

Si, R., Guo, S., Dai, Q., 2017. Durability performance of rubberized mortar and concrete with NaOH-Solution treated rubber particles. Construction and Building Materials 153, 496-505.

Si, R., Wang, J., Guo, S., Dai, Q., Han, S., 2018. Evaluation of laboratory performance of self-consolidating concrete with recycled tire rubber. Journal of Cleaner Production 180, 823-831.

Skarżyński, Ł., Suchorzewski, J., 2018. Mechanical and fracture properties of concrete reinforced with recycled and industrial steel fibers using Digital Image Correlation technique and X-ray micro computed tomography. Construction and Building Materials 183, 283-299.

Sukontasukkul, P., Pongsopha, P., Chindaprasirt, P., Songpiriyakij, S., 2018. Flexural performance and toughness of hybrid steel and polypropylene fibre reinforced geopolymer. Construction and Building Materials 161, 37-44.

Thomas, B.S., Chandra Gupta, R., 2016. Properties of high strength concrete containing scrap tire

rubber. Journal of Cleaner Production 113, 86-92.

Thomas, B.S., Gupta, R.C., 2016. A comprehensive review on the applications of waste tire rubber in cement concrete. Renewable and Sustainable Energy Reviews 54, 1323-1333.

Thomas, B.S., Gupta, R.C., Panicker, V.J., 2016. Recycling of waste tire rubber as aggregate in concrete: durability-related performance. Journal of Cleaner Production 112, 504-513.

Tu, W., Zhu, Y., Fang, G., Wang, X., Zhang, M., 2019. Internal curing of alkali-activated fly ash-slag pastes using superabsorbent polymer. Cement and Concrete Research 116, 179-190.

Turatsinze, A., Bonnet, S., Granju, J.L., 2007. Potential of rubber aggregates to modify properties of cement based-mortars: Improvement in cracking shrinkage resistance. Construction and Building Materials 21(1), 176-181.

Wongsa, A., Sata, V., Nematollahi, B., Sanjayan, J., Chindaprasirt, P., 2018. Mechanical and thermal properties of lightweight geopolymer mortar incorporating crumb rubber. Journal of Cleaner Production 195, 1069-1080.

Yang, K.-H., Song, J.-K., Song, K.-I., 2013. Assessment of CO2 reduction of alkali-activated concrete. Journal of Cleaner Production 39, 265-272.

Yousefieh, N., Joshaghani, A., Hajibandeh, E., Shekarchi, M., 2017. Influence of fibers on drying shrinkage in restrained concrete. Construction and Building Materials 148, 833-845.

Zamanzadeh, Z., Lourenço, L., Barros, J., 2015. Recycled Steel Fibre Reinforced Concrete failing in bending and in shear. Construction and Building Materials 85, 195-207.

Zhang, Z., Zhu, Y., Yang, T., Li, L., Zhu, H., Wang, H., 2017. Conversion of local industrial wastes into greener cement through geopolymer technology: A case study of high-magnesium nickel slag. Journal of Cleaner Production 141, 463-471.

Zhou, B., Uchida, Y., 2017. Influence of flowability, casting time and formwork geometry on fiber orientation and mechanical properties of UHPFRC. Cement and Concrete Research 95, 164-177.

Figures

Fig. 1. Raw materials used in this study: (a) FA; (b) GGBS; (c) sand; (d) 2-6 mm CR; (e) 12 mesh (i.e. 1.68 mm) CR; (f) 30 mesh (i.e. 0.595 mm) CR

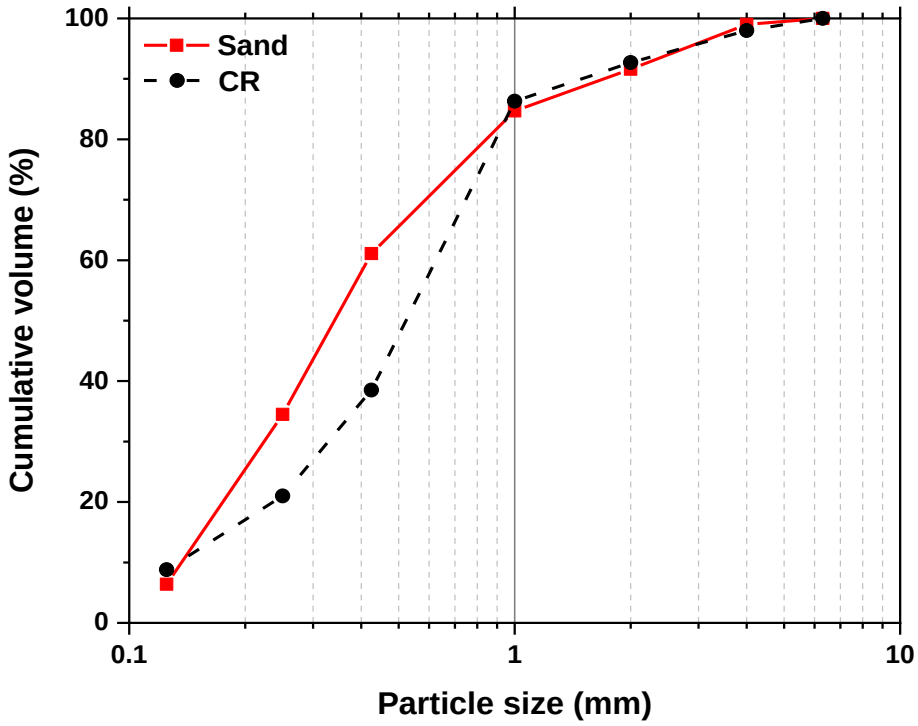

Fig. 2. Particle size distribution of sand and crumb rubber (CR)

Fig. 3. Recycled tyre steel fibre (RTSF): (a) picture; (b) image taken by digital microscope (Dino-Lite Edge AM73115MZT)

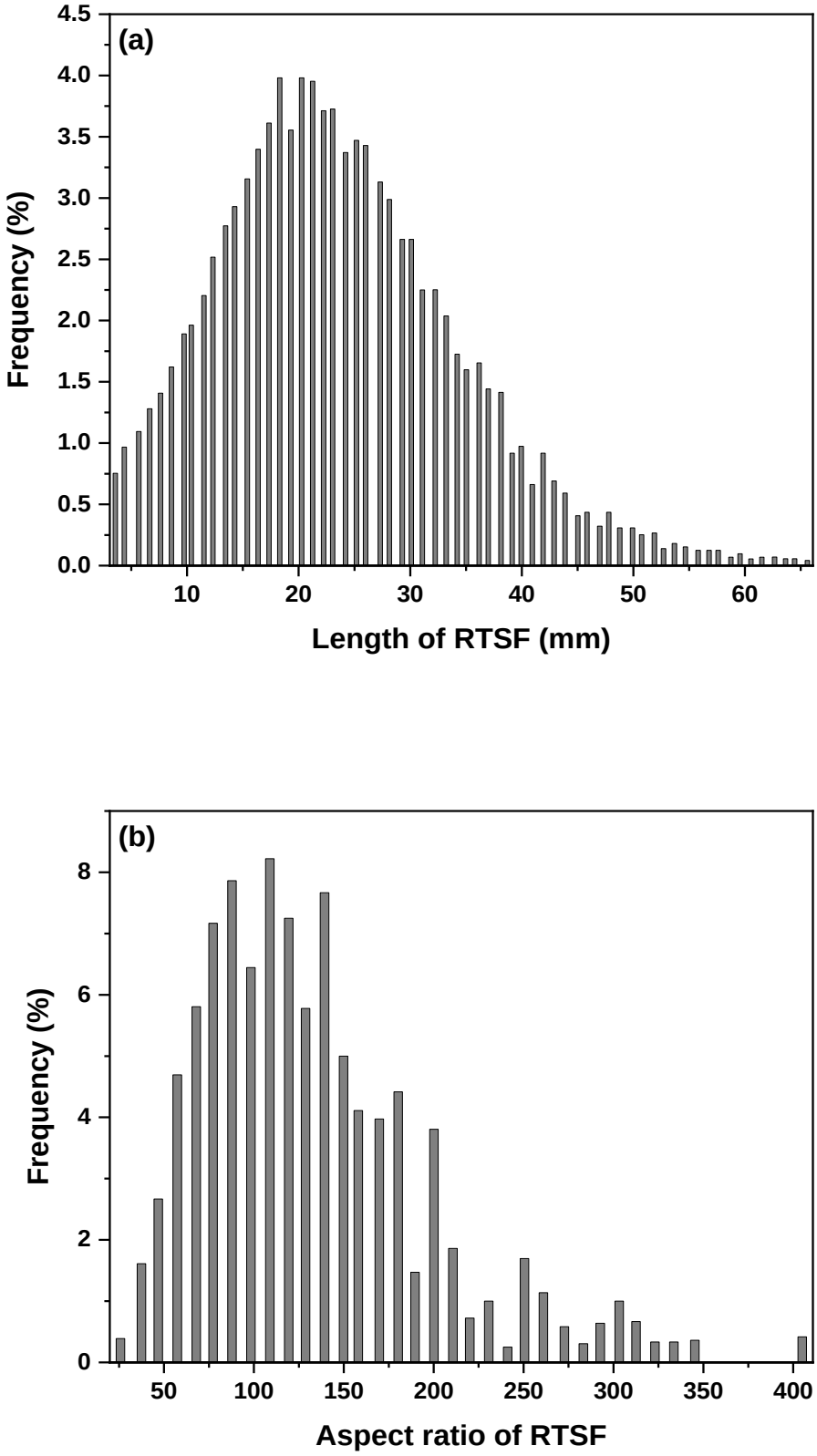

Fig. 4. Distributions of RTSF: (a) fibre length; (b) fibre aspect ratio (reproduced from Hu et al., 2018)

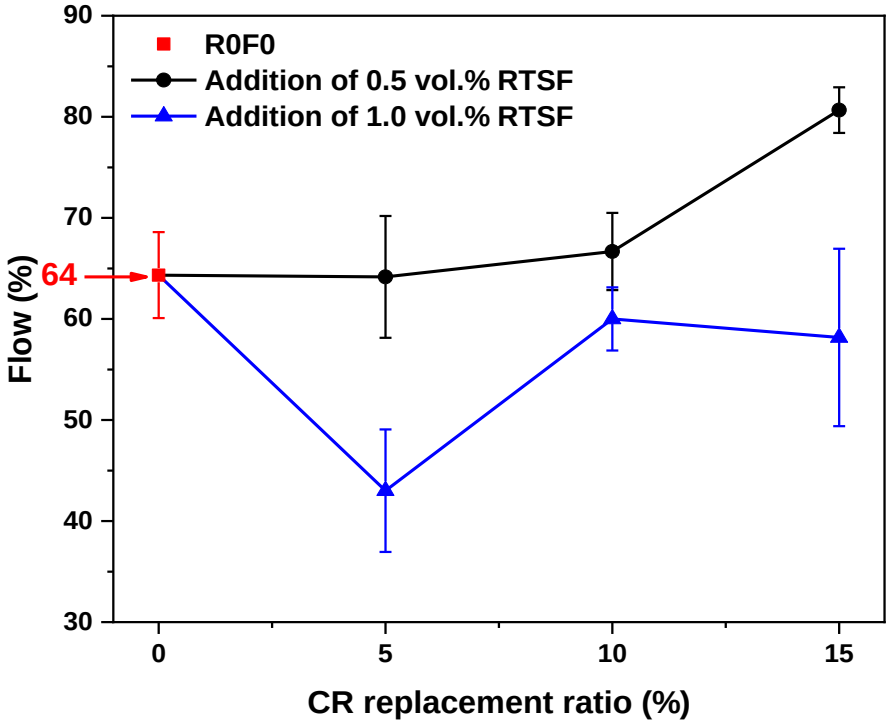

Fig. 5. Effects of CR and RTSF on flow value of all mixtures

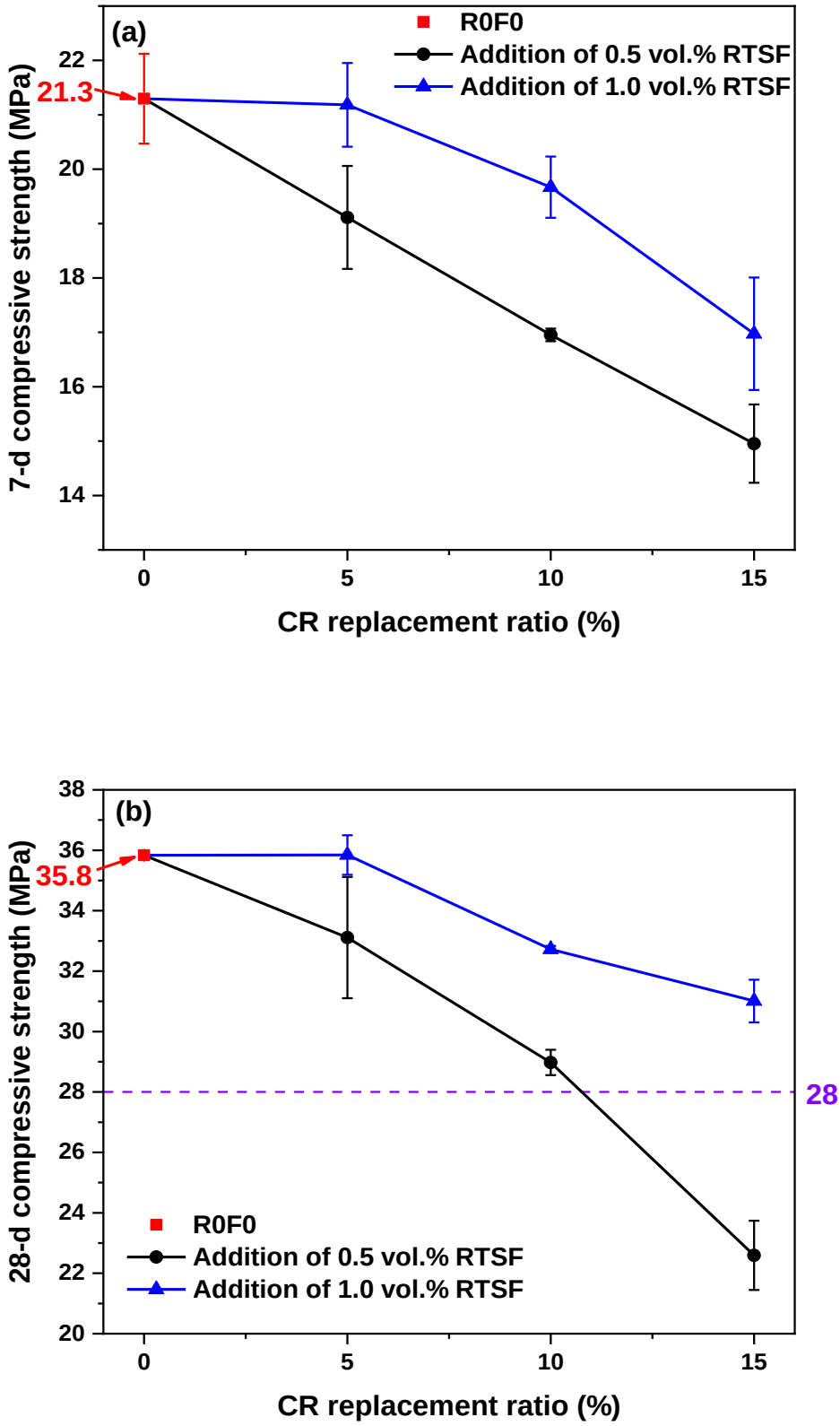

Fig. 6. Effects of CR and RTSF on compressive strength of all mixtures: (a) 7 d; (b) 28 d

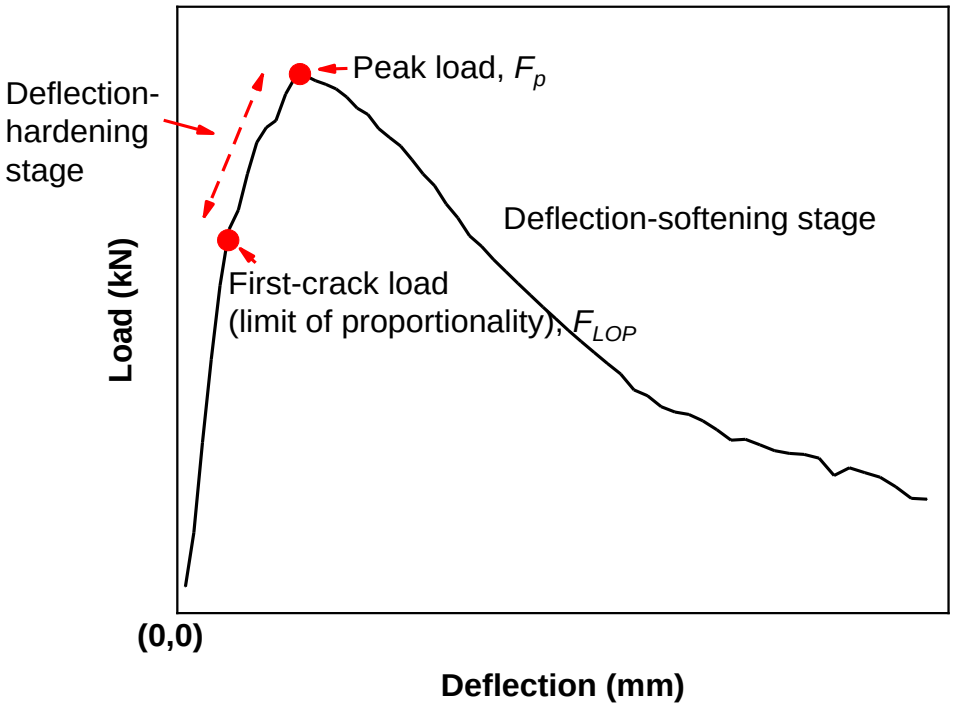

Fig. 7. Typical stages of load-deflection curve for fibre reinforced concrete

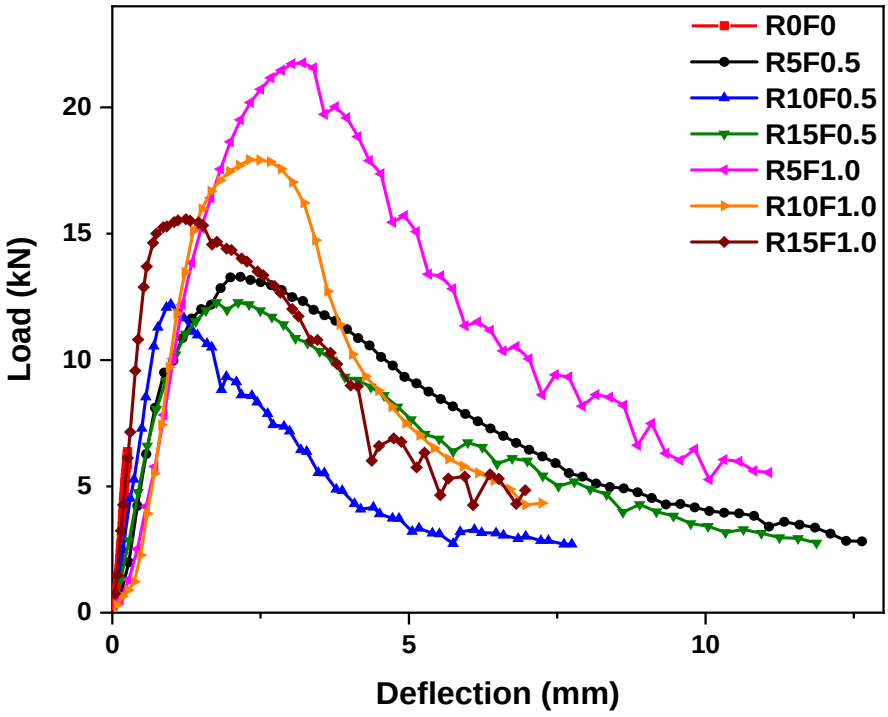

Fig. 8. Load-deflection curve of all mixtures under four-point bending

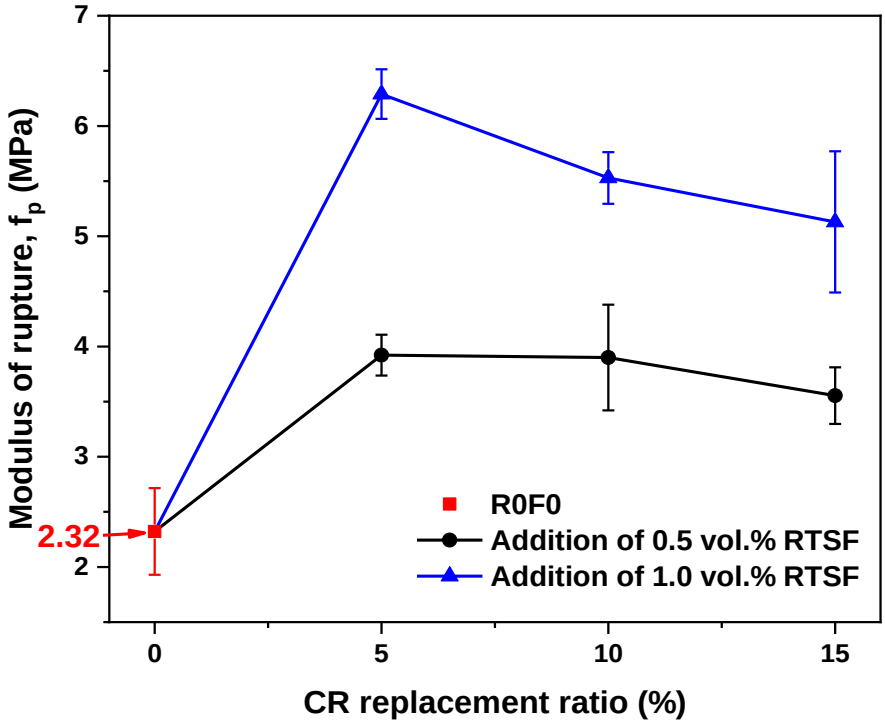

Fig. 9. Effects of CR and RTSF on 28-d modulus of rupture (flexural strength) of all mixtures

Fig. 10. Typical crack propagation of RSFRAM under four-point bending and post-failure crack pattern near midspan

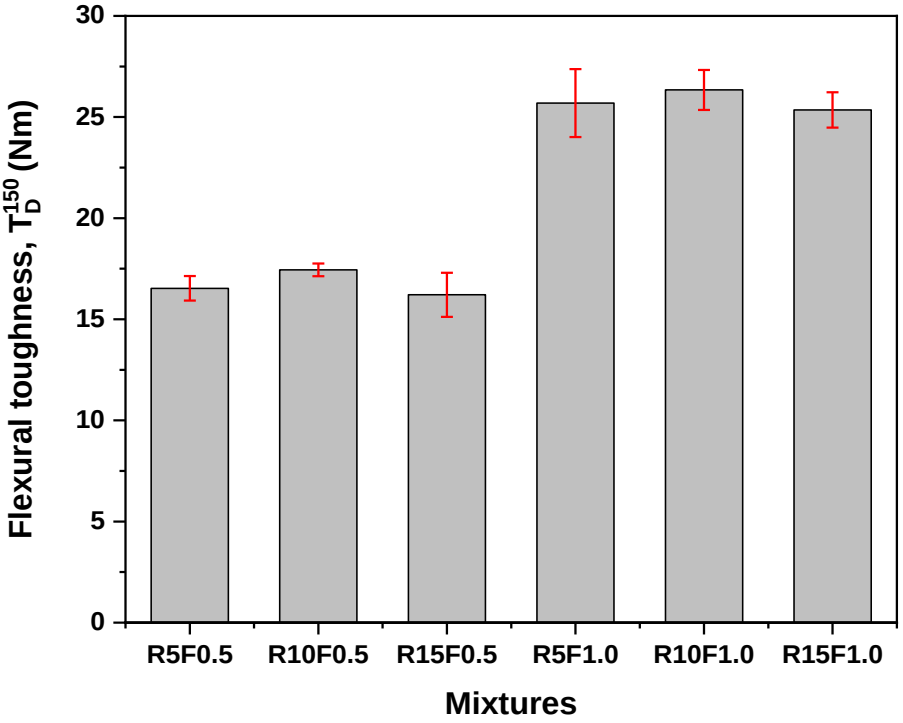

Fig. 11. Flexural toughness of all RSFRAM mixtures

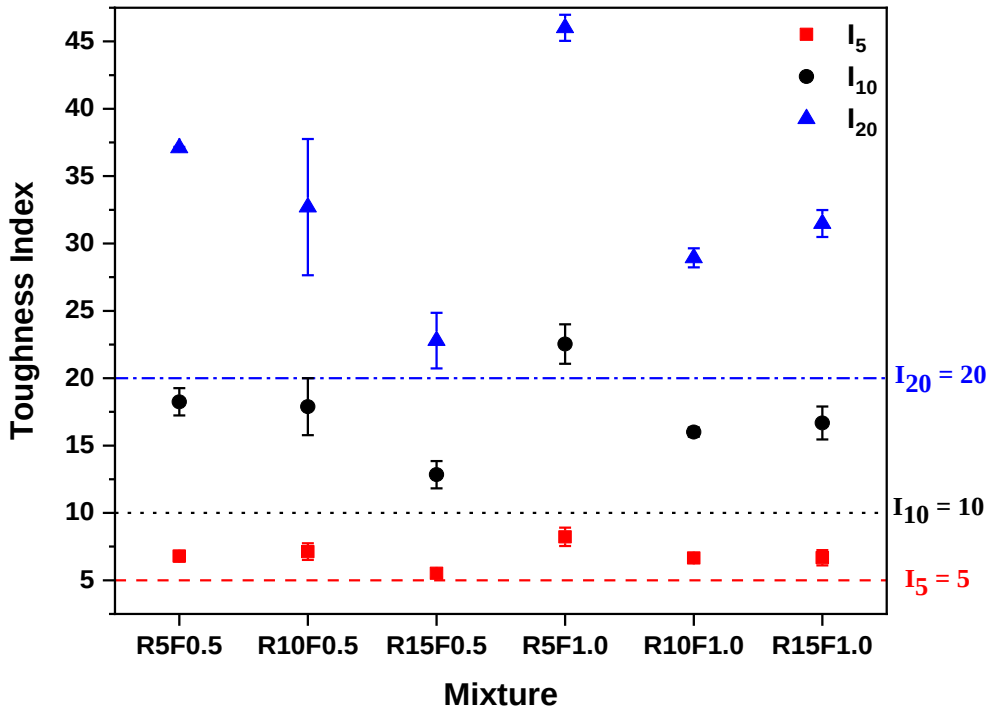

Fig. 12. Toughness indices I_5, I_{10} and I_{20} of all RSFRAM mixtures

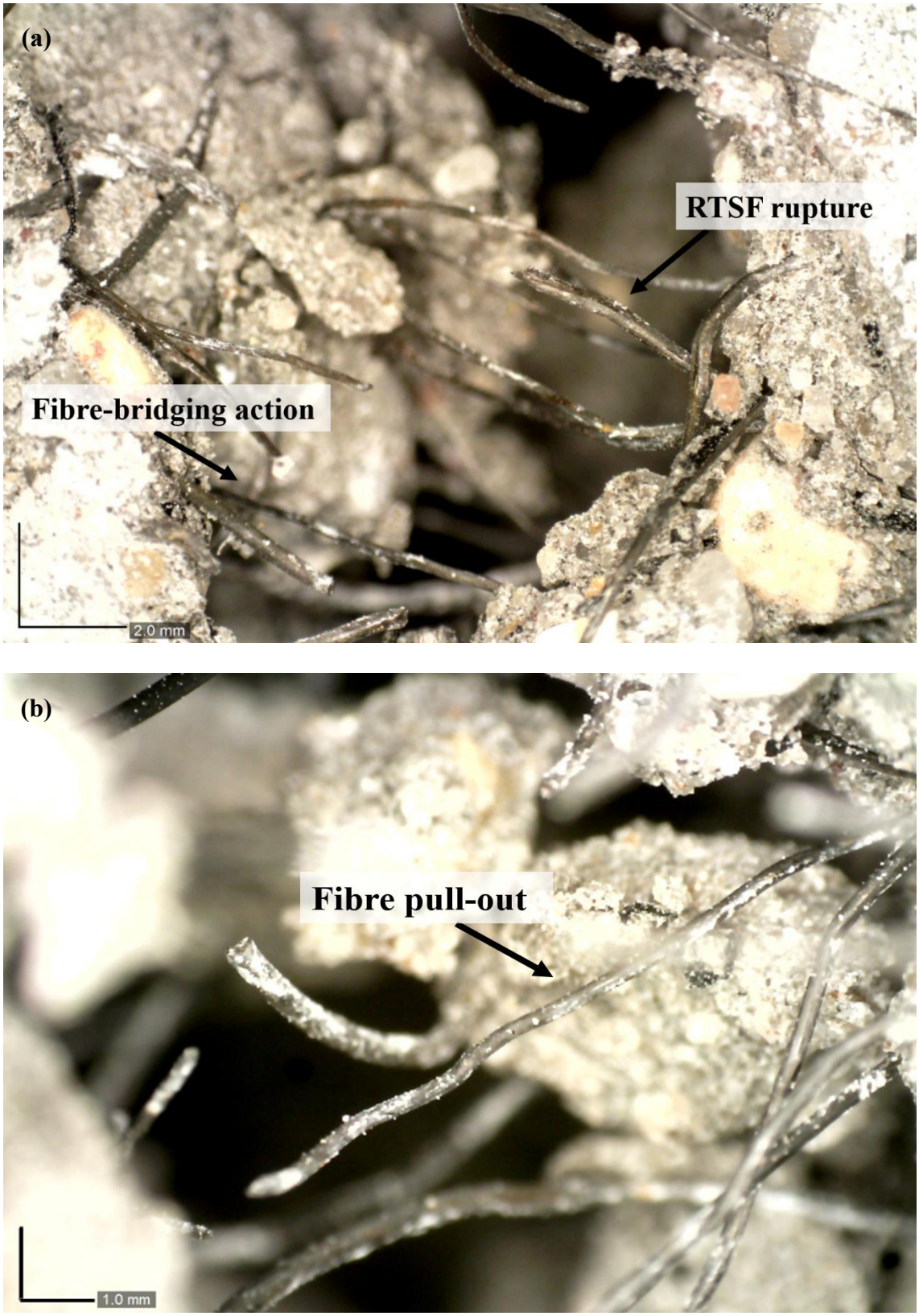

Fig. 13. Crack details of (a) RSFRAM with 0.5 vol.% RTSF addition; (b) RSFRAM with 1.0 vol.% RTSF addition

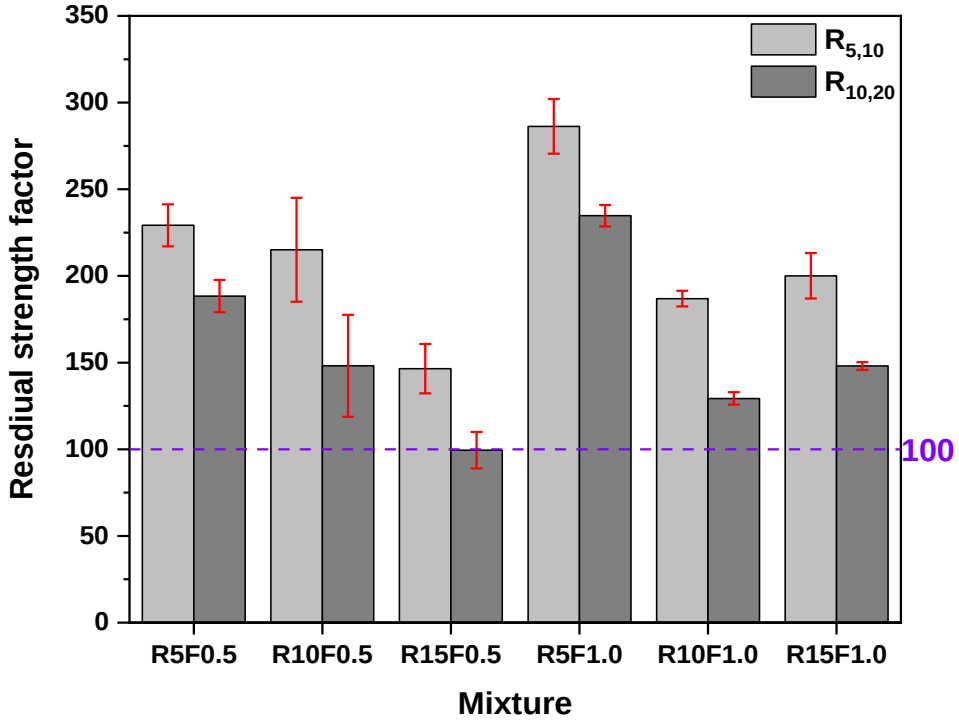

Fig. 14. Residual strength factors $R_{5,10}$ and $R_{10,20}$ of all RSFRAM mixtures

Fig. 15. Example of failed sections of a RSFRAM sample with 1.0 vol.% RTSF addition

Tables

Table 1. Chemical compositions (wt%) of FA and GGBS

Oxide	SiO_2	Al_2O_3	Fe_2O_3	K_2O	CaO	MgO	TiO_2	SO_3	MnO
FA	50.30	22.90	8.17	3.55	3.38	2	1.15	0.58	0.08
GGBS	34.10	12.30	0.41	0.56	44.20	8.12	0.96	2.59	0.25

Note; FA (fly ash); GGBS (ground granulated blast-furnace slag)

Table 2. Properties of RTSF used in this study

Fibre type	Length (mm)	Diameter (mm)	Aspect ratio	Tensile strength (MPa)	Elastic modulus (GPa)
RTSF	23	0.22	100	2570	200

Note: RTSF (recycled tyre steel fibre)

Table 3. Mixture proportions of AAFS mortars (kg/m^3)

Symbol	FA	GGBS	SS	SH	SPs	CR	RTSF	Sand
R0F0	320.0	80.0	106.7	53.3	4	0	0	800.0
R5F0.5	320.0	80.0	106.7	53.3	4	17.5	39.0	760.0
R10F0.5	320.0	80.0	106.7	53.3	4	35.1	39.0	720.0
R15F0.5	320.0	80.0	106.7	53.3	4	52.6	39.0	680.0
R5F1.0	320.0	80.0	106.7	53.3	4	17.5	78.0	760.0
R10F1.0	320.0	80.0	106.7	53.3	4	35.1	78.0	720.0
R15F1.0	320.0	80.0	106.7	53.3	4	52.6	78.0	680.0

Note: SS (sodium silicate); SH (sodium hydroxide); SPs (superplasticizers); CR (crumb rubber)